Hindawi Publishing Corporation
International Journal of Optics
Volume 2014, Article ID 865814, 9 pages
http://dx.doi.org/10.1155/2014/865814

Research Article

Optical Properties of Malachite Green Dye Doped SiO_2 Glasses: Effect of Transition Metal (Fe-I) Used as a Codopant

Dulen Bora and Subrata Hazarika

Assam University, Diphu Campus, Karbi Anglong, Assam 782462, India

Correspondence should be addressed to Dulen Bora; dulen.bora@gmail.com

Received 6 January 2014; Accepted 12 April 2014; Published 22 May 2014

Academic Editor: Sulaiman Wadi Harun

Enhanced luminescence properties of Malachite Green (MG) (oxalate) in Fe-MG codoped SiO_2 glasses compared to its values in MG doped SiO_2 glasses are reported here. The enhancement is chiefly attributed to a resonance nonradiative energy transfer between Fe and MG. The quantum yield of Malachite Green (MG), in presence of Iron, trapped in sol-gel derived SiO_2 glass increases by an order of ~10^3 compared to that in low viscous solvent while a lifetime of 3.29 ns is reported.

1. Introduction

Different groups of elements used as dopant and/or codopant often redefine and modify material properties of chemically compatible solid matrices. Tuning of band gap in materials for application in solar cells, inducing extrinsic conductivity in semiconductors, evolution of critical temperature TC in superconductivity or colossal magneto resistivity [1], and enhancement in luminescence properties of lanthanide doped materials [2] are few examples. Amongst various elements used as dopant and/or codopant, transition metal (TM) elements offer specific advantage. Codoping of TM improves photocatalytic activity of *n*-type metal oxide semiconductors [3], changes optical properties and photoactivity of nanoparticulates [4], influences the broad band luminescence excitation mechanism in rare earth-doped glasses [5], quenches lanthanide (Nd^{3+}) transitions in glasses [6], and so forth. TM oxide semiconductors are codoped with other elements to stabilize their magnetic properties [7]. Besides the effect of codopant elements, luminescence properties of materials also depend on the host structure and other chemical constituents of the host. Luminescence intensity and quantum yield of organic molecules and chromophore dyes when trapped in porous solid matrices are increased by several orders compared to their values in liquid solvent. As such, laser dyes doped in solid porous matrices are extensively used in the development of solid state dye lasers [8]. But, to our knowledge, very few works are reported on codopant effect on luminescence properties of dyes under confinement of solid matrices and none with transition metal as codopant. The study of energy transfer in silica xerogel codoped with Coumarin-120 dye and lanthanide ions, namely, Eu^{3+} and Tb^{3+} [9], and in thorium phosphate xerogel codoped with Coumarin-460 dye and Tb^{3+} [10] and Eu^{3+} [11] is an example of some of such reported works. It is, therefore, rightly said that the potential of doping/codoping of sol-gel derived glasses and similar materials with both lanthanide and transition metal elements is yet to be fully explored [12].

In this paper, the effect of codoping transition metal (Fe-I) on optical properties of Malachite Green (MG) oxalate dye trapped in the pores of sol-gel derived silica glasses via doping is investigated with emphasis on photoluminescence properties. MG (oxalate) dye is a member of the triarylmethane group with low quantum yield, which is increased by ~10^3 times the values reported [13] in low-viscous liquid solvents when doped in solid silica matrices.

2. Materials and Methods

2.1. Preparation of Fe-MG Codoped SiO_2 Glasses. Tetraethylorthosilicate (TEOS) and Malachite Green (oxalate) from Merck and methanol, doubly distilled water, nitric acid, and Iron filings (Fe-I) from Rankem were used in preparation of

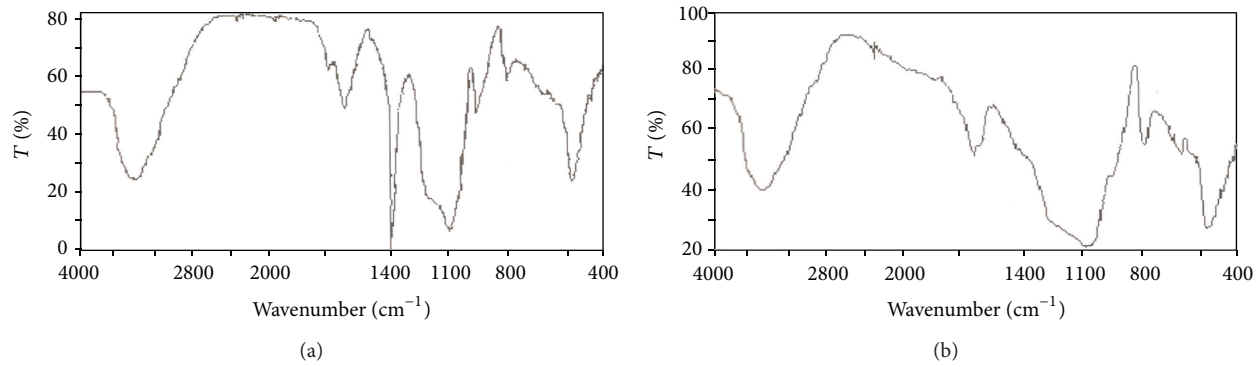

Figure 1: (a) IR-spectra of MG-Fe doped (F3M1) glass (air dried). (b) IR-spectra of MG-Fe doped (F3M1) glass (heat treated at 150°C).

Fe-MG codoped SiO_2 glasses. In all, eight codoped glasses labelled FxMy (x = 1–4 and y = 1, 4) and two MG doped glasses labelled Mx (x = 1, 4) were prepared for this investigation by varying the concentration of Fe and MG. In FxM1 (x = 1–4) glasses MG concentration was kept at 1×10^{-5} M and the varying Fe concentration was 0.01 M (in F1M1 glass), 0.02 M (in F2M1 glass), 0.03 M (in F3M1 glass), and 0.04 M (in F4M1 glass). In FxM4 (x = 1–4) glasses the concentration of MG was 5×10^{-4} M and codopant concentration was varied as in the earlier set. In M1 and M4 glasses the MG concentrations were 1×10^{-5} M and 5×10^{-4} M, respectively. In preparation of Fe-MG codoped SiO_2 glasses by sol-gel technique, a solution of tetraethylorthosilicate (TEOS) in methanol—the metal alkoxide—was polymerized under catalyst action of doubly distilled water and dilute nitric acid. The process being a low temperature synthesizer of glass facilitated the use of volatile dopants like chromophore dyes without destruction of their characteristics [14, 15]. Initially, requisite quantity of MG and Fe or MG alone (as per requirement of type of glass) was dissolved in 10.5 mL mixture of methanol (8.75 mL), distilled water (1.25 mL), and dilute nitric acid (0.5 mL) taken in proportion of 70 (Methanol) : 10 (H_2O) : 4 (HNO_3) parts by stirring continuously for 15 min in a magnetic stirrer with teflon coated stirrer bar. At this point 2 mL of TEOS, which forms the remaining 16 parts in a total mixture of 12.5 mL solvent, was added (to the mixture in the stirrer) and further stirred for 1 hr. As the formation of gel began the entire mass of gel was poured into plastic structure (shell) and left to dry and solidify at room temperature (25–27°C). With progress in hydrolysis the gel solidified to form coloured stiff hard mass pellet (xerogel/sol-gel glass) in 48–72 hrs. The colour of the glass was imparted by the dye molecules entrapped in the pores of the xerogel/sol-gel glass. Initially, just after the formation of xerogel via hydrolysis and polycondensation, the colour of the glass remained green (the same as the colour of Malachite Green in solution) which turned deep orange with ageing of the sol-gel glass.

2.2. Instruments and Methods. IR spectra in the range 4000–400 cm^{-1} were recorded using KBr technique with a Jasco FT/IR 300E spectrophotometer. VIS absorption spectra of the glasses in the range of 400–700 nm were recorded in UV-VIS-NIR spectrophotometer (CARY-5E) and their photoluminescence spectra were taken in a JY Fluorolog-3-11 spectrofluorometer, excited by 445 nm wavelength of a 450 W Xenon lamp, keeping slit width at 5 nm, with integration time 0.1 s and step size 1 nm. Fluorescence lifetime measurements of four glasses, namely, M1, M4, F3M1, and F3M4 at λ_{em} = 573 nm, 585 nm, 628 nm, and 624 nm, respectively, were performed in FluoroCube —a lifetime measurement system from HORIBA. The instrument response function (IRF) of the instrument was 1.263 ns obtained using LUDOX SM-30 colloidal suspension in water. The excitation source for lime time measurement was a 460 nm LED. TEM micrographs of four MG doped SiO_2 glass matrices with and without Fe-I codopant were recorded in a JEOL JEM-2100 ultrahigh resolution TEM. All measurements and recordings were done in room temperature (25–27°C).

3. Results and Discussion

3.1. Structural Analysis

IR Spectra: Structure-Composition Relation of Matrix. IR-absorption spectra of MG-Fe doped sol-gel glass F3M1 are shown in Figures 1(a) and 1(b), respectively. IR absorption spectroscopy using KBr technique is successful in study of structure-composition relation in glasses and ceramics [16]. Moreover, it can be used to identify low concentration impurities, such as water and hydroxyl ions in glasses [17].

The fingerprint region of the IR spectra in Figures 1(a) and 1(b) is predominated by bands associated with network vibrational modes of Si-O-Si and Si-O groups. Strong and intense band due to Si-O-Si asymmetric stretching appears around 1088 cm^{-1} and due to its bending mode at around 464 cm^{-1} (with a shoulder at around 549 cm^{-1}). The weak band at around 797 cm^{-1} may be assigned to Si-O-Si symmetric stretching of the bridging oxygen. The band around 969 cm^{-1} may be assigned to Si-O stretching with one or two nonbridging oxygens [18]. Besides, at around 1384 cm^{-1} a strong and intense band is attributed to vibration of TEOS, ethoxy group (due to CH_3 symmetric bending) [19]. This band is very unstable and disappears on application of heat.

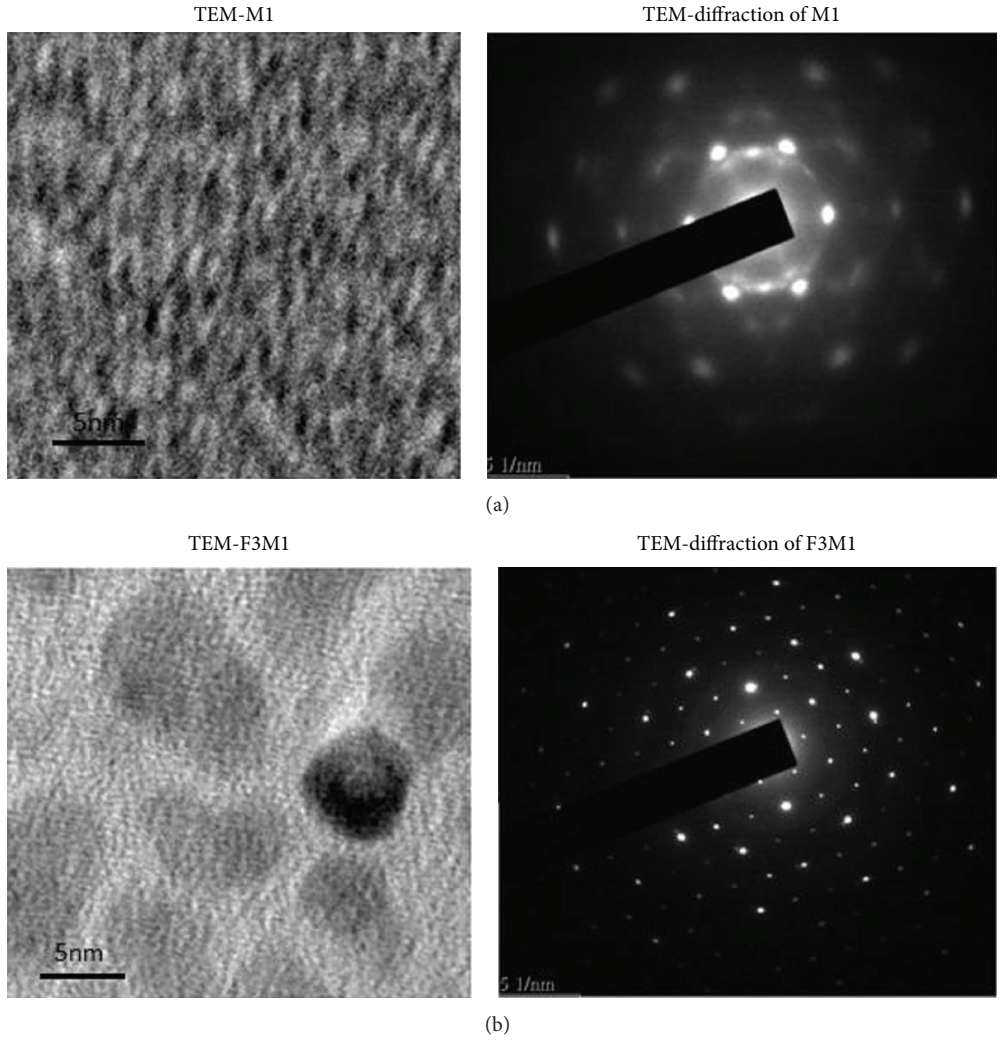

Figure 2: (a) TEM micrograph of MG doped (M1) glass with its diffraction pattern. (b) TEM micrograph of MG-Fe doped (F3M1) glass with its diffraction pattern.

The fact is reflected in the IR spectra in Figure 1(b) of F3M1 glass recorded after heat treatment at 150°C. The very strong and broad band on the higher wave number side of the spectra, that is, around 3461 cm^{-1}, corresponds to the fundamental vibrations of –OH groups and indicates strong presence of hydroxyl groups in the glass. Similarly, the band around 1634 cm^{-1} assigned to bending modes of water molecules indicates strong presence of adsorbed water.

TEM Micrographs and Diffraction Pattern of Matrices. Transmission electron micrographs (TEM) and their diffraction patterns of the MG doped and MG-Fe codoped silica matrices are presented in Figures 2(a) and 2(b) which clearly reveal the variation in morphological structure of matrices with Fe-I codopant. Appearance of TEM diffraction pattern reflects the nature of phases of the specimens. Patterns of microcrystalline or amorphous matrices like polymers and metallic glasses, that lack long range order in atomic lattice, consist of concentric rings [20]. Diffraction ring patterns marked by reflection spots, as in F1M1 glass, often refer to matrices formed by large collection of crystallites with different orientations. The individual reflections from such crystals appear as spots on the rings.

3.2. Spectral Analysis

Absorption and Emission Spectra. Effect of Fe-I on the absorption and photoluminescence properties of MG in SiO_2 sol-gel derived glasses is studied for 1×10^{-5} M (M1 glass) and 5×10^{-4} M (M4 glass) concentrations of MG. Their spectra along with variations in absorbance and photoluminescence intensity with Fe-I concentration between 0.01 M and 0.04 M in the glasses are presented in Figures 3(a), 3(b), 4(a), 4(b), 5(a), 5(b), 6(a), and 6(b), respectively.

Absorption Bands I and II undergo red shift and show enhancement in their absorbance compared to their values in SiO_2 glasses. Resolution of Band II is vastly improved with its spectral features becoming sharper and well defined. The absorption maxima of MG (Peak I) at 441 nm and 447 nm in glasses with 1×10^{-5} M and 5×10^{-4} M concentrations

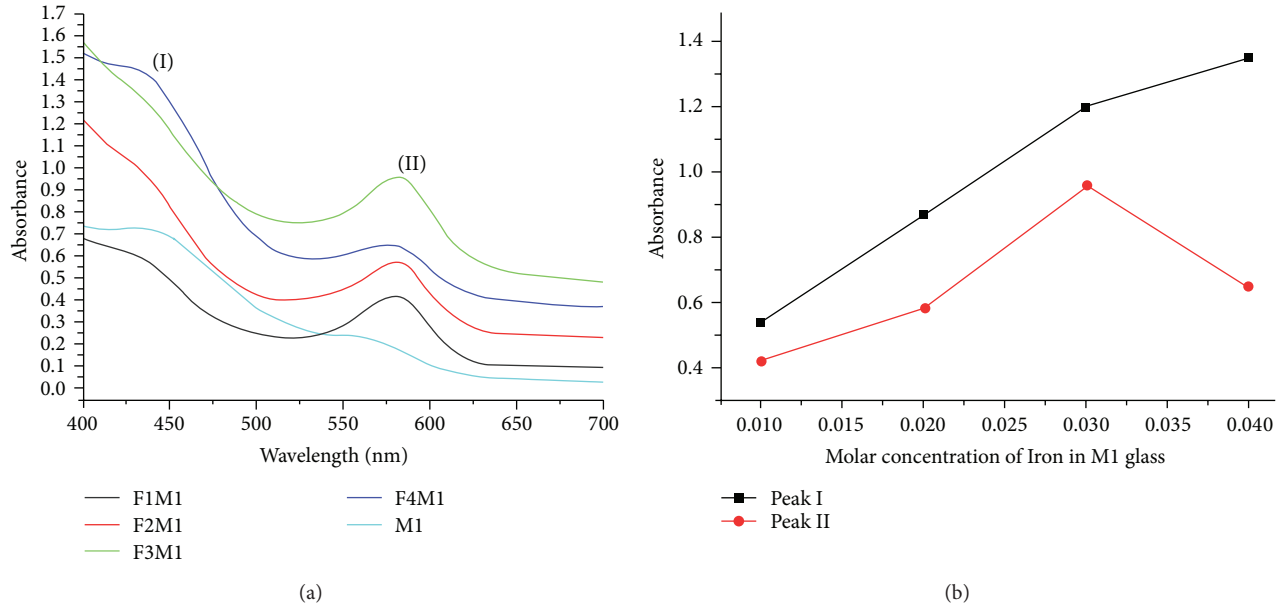

Figure 3: (a) Absorption spectra of Fe-MG SiO_2 glasses (F1M1, F2M1, F3M1, and F4M1) and M1 glass. (b) Variation of absorbance with molar concentration of Fe-I in FxM1 glasses (x = 1–4).

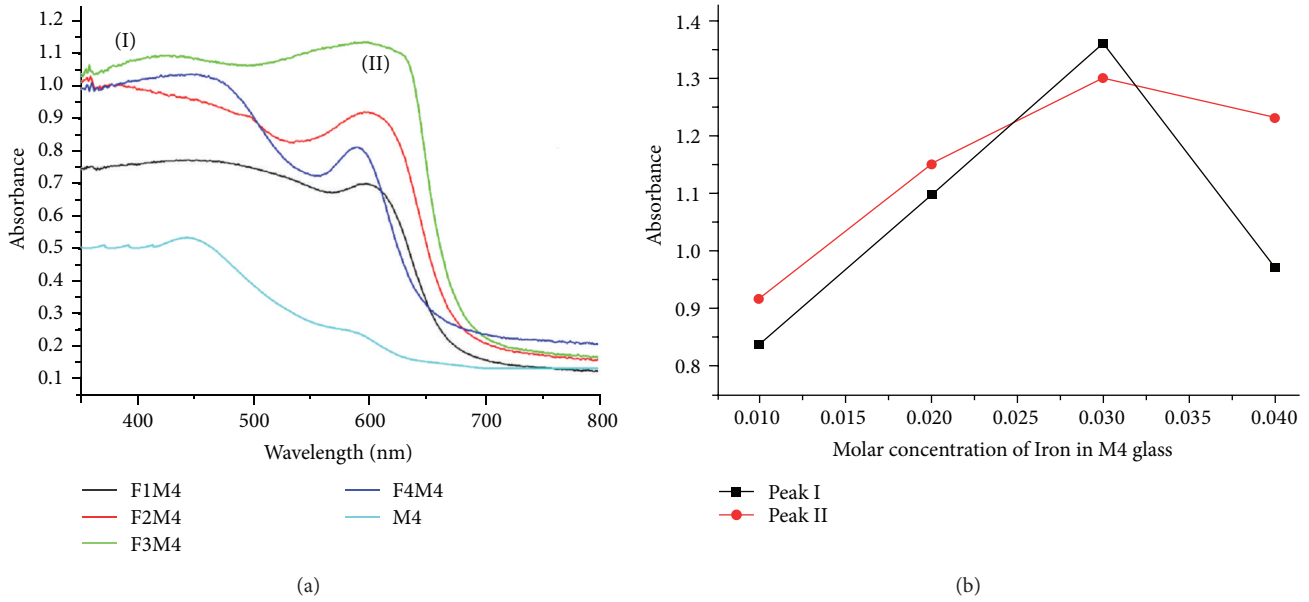

Figure 4: (a) Absorption spectra of Fe-MG SiO_2 glasses (F1M4, F2M4, F3M4, and F4M4) and M4 glass. (b) Variation of absorbance with molar concentration of Fe-I in FxM4 glasses (x = 1–4).

in presence of 0.03 M of Fe-I are red shifted by ~6 nm and ~10 nm, respectively, with a corresponding increase in absorbance by 73.3% and 90.9%, respectively. In FxM1 (x = 1–4) and FxM4 (x = 1–4) glasses the absorbance of Band I increases linearly with Fe concentration up to 0.03 M and accounts for an additional increase of 34 M^{-1} cm^{-1} and 27 M^{-1} cm^{-1} in the molar extinction coefficient (ε) of MG in FxM1 (x = 1–4) and FxM4 (x = 1–4) glasses, respectively. Similar variation in absorbance with Fe concentration is absent for Band II. The best resolved spectral profile amongst FxM4 (x = 1–4) glasses is observed for the glass with x = 4, though with a reduced absorbance. Absorption in M1 glass at 441 nm obeyed Beer-Lambert's law while at M4 glass it is deviated. Oscillator strengths of the absorption bands in presence of Fe are determined from integrated absorption coefficients using the formula

$$f = 4.32 \times 10^{-9} \int \varepsilon(v)\, dv, \quad (1)$$

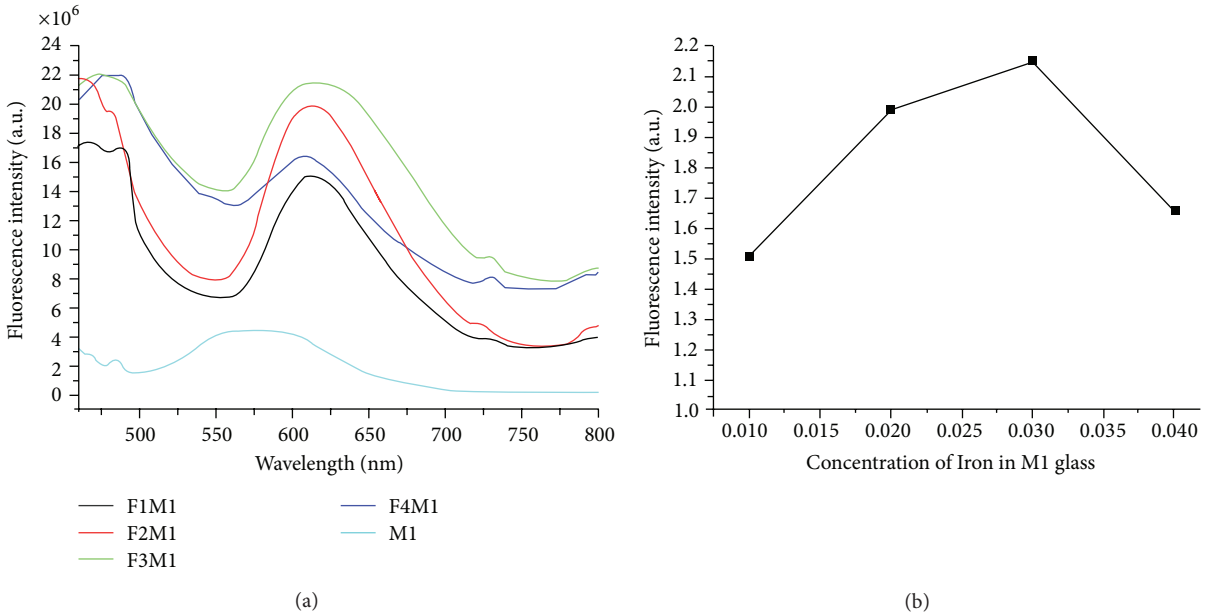

FIGURE 5: (a) Photoluminescence spectra of Fe-MG SiO_2 glasses (F1M1, F2M1, F3M1, and F4M1) and M1 glass. (b) Variation of photoluminescence intensity with molar concentration of Fe-I in FxM1 glasses (x = 1–4).

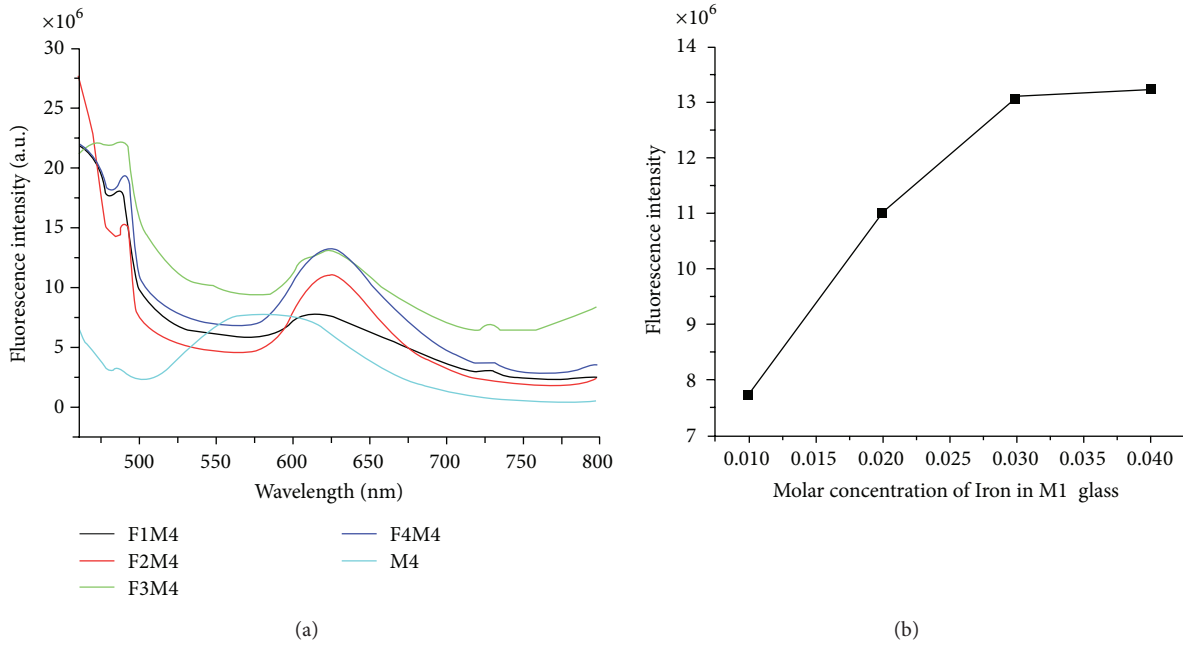

FIGURE 6: (a) Photoluminescence spectra of Fe-MG SiO_2 glasses (F1M4, F2M4, F3M4, and F4M4) and M4 glass. (b) Variation of photoluminescence intensity with molar concentration of Fe-I in FxM4 glasses (x = 1–4).

where $\int \varepsilon(\upsilon)d\upsilon \approx \varepsilon(\upsilon) \times \Delta\upsilon$ and $\varepsilon(\upsilon)$ is the molar absorption coefficient at frequency $\upsilon(\text{cm}^{-1})$ and $\Delta\upsilon$ is the band width at $1/2\varepsilon(\upsilon)$ measured directly from absorption spectra (FWHM) "Origin-8.5" software. These values of MG-Fe doped glasses are much reduced compared to their corresponding values in M1 and M4 glasses. This is due to a reduction in its $\Delta\upsilon$ values of the bands in codoped glasses. The calculated oscillator strength of the absorption bands together with absorbance maxima wavelength ($\lambda_{(\text{abs})}$) and FWHM of the bands are compiled in Table 1 for comparison. Presence of small quantities of Fe-I in vicinity of MG molecules in the matrix can lower site symmetry around the molecule and could have resulted in increased absorbance in these codoped glasses. Codopants like Al and P are known to cause such enhancement in absorbance of lanthanide transitions in doped glasses [21]. A possible cause of deviation

Table 1

Sample code	MG conc. ($\times 10^{-5}$) M	Fe conc. M	[a]Peak abs. WL (λ_{abs}) nm	[b]Oscillator strength (f)	[c]FWHM ($\Delta\upsilon$) cm^{-1}	[d]Abs. coeff. ($\varepsilon(\upsilon) \times 10^4$) $M^{-1}cm^{-1}$
FxM1 glass, x = 1–4						
			Peak I			
F1M1	1	0.01	443	0.556193	1608.67	8.0034
F2M1	1	0.02	442	0.579773	1676.87	8.0034
F3M1	1	0.03	447	0.552859	1599.03	8.0034
F4M1	1	0.04	448	0.993193	2872.89	8.0026
M1	1	0.00	441	3.932051	11377.46	8.0000
			Peak II			
F1M1	1	0.01	582	0.013727	1351.54	0.2351
F2M1	1	0.02	580	0.013571	1336.21	0.2351
F3M1	1	0.03	581	0.013726	1351.46	0.2351
F4M1	1	0.04	579	0.013773	1369.46	0.2328
M1	1	0.00	561	0.070586	7030.67	0.2324
FxM4 glass, x = 1–4						
			Peak I			
F1M4	50	0.01	450	0.534699	3238.52	3.8219
F2M4	50	0.02	456	0.695247	4210.91	3.8219
F3M4	50	0.03	422	0.647504	3921.74	3.8219
F4M4	50	0.04	466	0.43928	2661.22	3.8210
M4	50	0.00	447	7.633639	46257.75	3.8200
			Peak II			
F1M4	50	0.01	608	0.000186	1269.53	0.0035
F2M4	50	0.02	608	0.000259	1761.06	0.0035
F3M4	50	0.03	586	0.000357	2430.14	0.0035
F4M4	50	0.04	594	0.000048	923.38	0.0012
M4	50	0.00	591	0.000167	4838.51	0.0008

[a]Peak absorption wavelength (λ_{abs}); [b]oscillator strength (f) of absorption bands; [c]FWHM ($\Delta\upsilon$) of bands; and [d]molar absorption coefficient [$\varepsilon(\upsilon)$] of MG in Fe-MG doped SiO_2 sol-gel glasses.

of absorption from Beer-Lambert law and a subsequent decrease in absorbance in some cases at higher concentration of Fe-I (0.04 M) may be attributed to *shadow* effect, where the absorbing dye molecules are effectively screened from the incident radiation by presence of large quantity of Fe-I codopants in its path.

Addition of 0.01 M–0.03 M Fe-I significantly improves the luminescence properties of MG in these glasses. The photoluminescence bands of MG in SiO_2 glasses in presence of Fe-I under 445 nm excitation become narrower in width, sharper in profile, and with peak centres red shifted by ~ 55 nm and ~39 nm in FxM1 (x = 1–4) and FxM4 (x = 1–4) glasses, respectively. Photoluminescence intensity of MG with 0.03M concentration of Fe-I increases 4.8 and 1.72 times in FxM1 (x = 1–4) and FxM4 (x = 1–4) glasses, respectively, and intensities above it are saturated in F4M4 and quenched in F4M1 glasses, respectively.

Subsequently, measured values of quantum yield and radiative and nonradiative transition probabilities of MG in F3M1 and F3M4 glasses—where enhancement in luminescence intensity was best—are improved compared to its values in M1 and M4 glasses. The radiative (K_r) and nonradiative (K_{nr}) transition probabilities are calculated using the following relations [17]:

$$K_r = \frac{\phi}{\tau}, \qquad K_{nr} = \frac{(1-\phi)}{\tau}, \tag{2}$$

where ϕ and τ are measured fluorescence quantum yield (QY) and intrinsic decay time, respectively, of MG in the TEOS silica matrix used in this study. Fluorescence quantum yield (ϕ) is measured by comparison to a reference fluorophore [riboflavin] of known QY using the single point method by using the following equation:

$$\phi = \phi_r \frac{I}{I_r} \times \frac{OD_r}{OD} \times \frac{n^2}{n_r^2}. \tag{3}$$

In (3), ϕ_r is the quantum yield of the reference fluorophore. In these measurements riboflavin with ϕ_r = 0.3 is taken

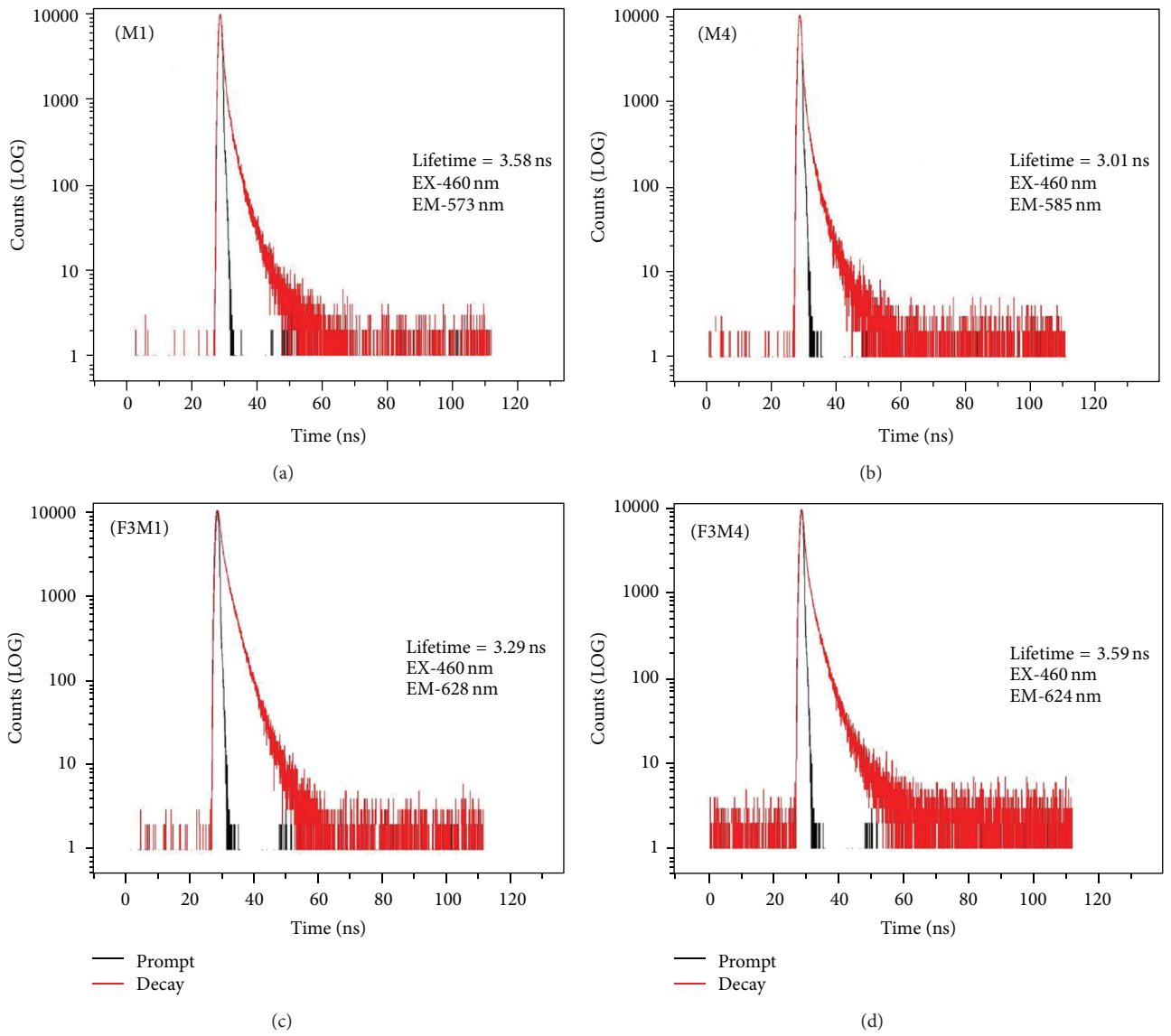

Figure 7: Photoluminescence decay curves of M1, M4, F3M1, and F3M4 glasses.

as the reference. "I" is the integrated fluorescence intensity and "OD" is the optical density. Subscript "r" refers to the reference fluorophore. Lifetime (τ) of excited MG states in SiO_2 glasses with and without codopants is estimated by double exponent iteration of the recorded decay curves. Its values do not show much variation on codoping with Fe-I. Decay curves recorded for M1, M4, F3M1, and F3M4 glasses are presented in Figure 7.

Photoluminescence properties derived using (2)-(3) for glasses F3M1, F3M4, M1, and M4 along with measured lifetime (τ) of excited states of MG, peak emission wavelength (λ_p), and effective band width ($\Delta\lambda_{\text{eff}}$) of luminescence bands are compiled in Table 2.

Confinement of organic molecules within rigid pores of a solid matrix restricts nonradiative routes for deactivation of excited molecules, resulting in an increase in photoluminescence intensity and quantum yield. Rigidity of the pores reduces space for rotational motion of the molecules and thereby limits nonradiative relaxation channels of excited trapped molecules. Codoping the confined organic chromophores/molecules [MG] with Fe-I leads to further filling up the pores, reducing free space, and increasing rigidity of the porous matrix and thereby photoluminescence intensity [22]. However, change in the matrix rigidity due to incorporation of Fe-I cannot solely account for an increase in photoluminescence intensity as in the present case. A significant contribution is from a resonance nonradiative energy transfer from Fe to MG. A strong spectral overlap observed between $a^5P_3 \rightarrow a^5D_4$ emission band of Fe-I at 567 nm (sensitizer) and $S_0 \rightarrow S_1$ MG absorbance band at 561 nm (activator) accompanied by increasing photoluminescence intensity of activator with donor concentration is indicative of such energy transfer. This Förster-Dexter [23, 24] kinetics governs resonance energy transfer and assumes random

Table 2

Sample code	MG conc. ($\times 10^{-5}$) M	Fe conc. M	[a]Peak Em. wavelength (λ_p) nm	[b]Effective bandwidth ($\Delta\lambda_{\text{eff}}$) nm	[c]QY (ϕ)	[d]Decay time (τ) ns	[e]Radiative trans. prob. (K_r) ($\times 10^8$) s^{-1}	[f]Nonradiative trans. prob. (K_{nr}) ($\times 10^8$) s^{-1}
				FxM1 glass, x = 1–4				
F1M1	1	0.01	620	66.93				
F2M1	1	0.02	621	76.39				
F3M1	1	0.03	628	85.06	0.13	3.29	0.40	2.63
F4M1	1	0.04	616	60.37				
M1	1	0.00	573	133.36	0.06	3.58	0.17	2.62
				FxM4 glass, x = 1–4				
F1M4	50	0.01	620	82.30				
F2M4	50	0.02	626	61.67				
F3M4	50	0.03	624	62.96	0.05	3.59	0.13	2.66
F4M4	50	0.04	626	64.94				
M4	50	0.00	585	132.69	0.07	3.01	0.21	3.09

[a]Peak emission wavelength (λ_p), [b]effective band width ($\Delta\lambda_{\text{eff}}$), [c]fluorescence quantum yield (ϕ), [d]radiative decay time (τ), [e]radiative rate (K_r), and [f]nonradiative transition probability (K_{nr}) of emission in Fe-MG doped SiO_2 glasses.

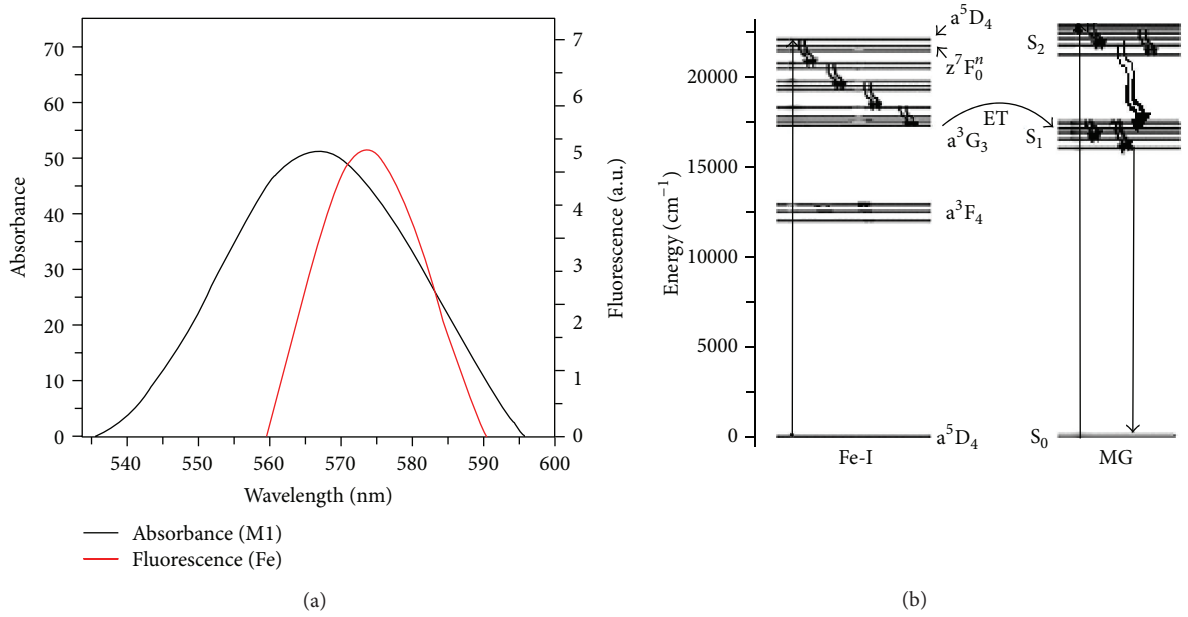

Figure 8: (a) Spectral overlap between $a^5P_3 \rightarrow a^5D_4$ emission band of Fe-I and $S_0 \rightarrow S_1$ MG absorbance band. (b) Schematic representation of energy transfer from Fe-I to MG dye in SiO_2 glass under 445 nm excitation.

and uniform distribution of sensitizer and activator where sensitizer-sensitizer interaction is considered to be absent. The energy transfer depends strongly on spectral overlap, emission cross-section of sensitizer, and absorption cross-section of activator expressed by critical distance

$$R_{SA}^6 = \frac{3c\tau_s}{8\pi 4n} \int \sigma_{\text{em}}^d(\lambda)\, \sigma_{\text{abs}}^a(\lambda)\, d\lambda. \quad (4)$$

Schematic representation of possible routes of energy transfer in Fe-Mg codoped SiO_2 glass under 445 nm excitation is presented in Figure 8. The transfer is accompanied by nonradiative loss to the matrix site that may have been expressed as vibration or heat because of which photoluminescence intensity increases nonlinearly with Fe-I concentration.

Further, TEM micrographs in Figure 2 along with diffraction patterns depict a transformation in silica matrix in presence of Fe-I and are indicative of a modification in the host ligand field acting on the vibrational levels of the trapped molecules causing a red shift [25] in the photoluminescence bands of Fe-MG codoped glasses. The comparatively homogeneous spectral features of these red shifted bands may be attributed to the changes in matrix structure.

4. Conclusion

A significant enhancement in photoluminescence intensity in Fe-MG codoped SiO_2 sol-gel glasses is observed which is attributed primarily to a resonance energy transfer from Fe to MG apart from increased rigidity of the pores, in which MG molecules are entrapped, due to codoping. Routes of energy transfer along with observed variations in transitions are also analysed. Intensity of the photoluminescence band in the MG doped SiO_2 glass with its peak centred (λ_p) at 573 nm and an effective bandwidth ($\Delta\lambda_{\text{eff}}$) of 133 nm is enhanced 4.8 times in presence of 0.03 M of Fe-I. Further, (λ_p) of the band is shifted towards red by 55 nm and ($\Delta\lambda_{\text{eff}}$) becomes narrower by 48 nm. The quantum yield of MG in presence of Fe-I is increased 2.16 times. The improvement in various radiative parameters needs to be examined in context of the effect of codopants from other groups, like Al—a commonly used codopant to sensitize luminescence efficiency in order to understand the effectiveness of Fe-I as a sensitizer of MG luminescence.

Conflict of Interests

The authors declare that there is no conflict of interests regarding the publication of this paper.

Acknowledgments

The authors render their sincere thanks to SAIF-IIT (Madras) and SAIF (NEHU) Shillong, for providing absolute support in instrumentation facilities for sample analysis.

References

[1] P. Mallick and N. C. Mishra, "Evolution of structure, microstructure, electrical and magnetic properties of nickel oxide (NiO) with transition metal ion doping," *The American Journal of Materials Science*, vol. 2, no. 3, pp. 66–71, 2012.

[2] C. Armellini, M. Ferrari, M. Montagna, G. Pucker, C. Bernard, and A. Monteil, "Terbium(III) doped silica-xerogels: effect of aluminum(III) co-doping," *Journal of Non-Crystalline Solids*, vol. 245, pp. 115–121, 1999.

[3] Z. Shi, H. Lai, S. Yao, and S. Wang, "Photocatalytic activity of Fe and Ce co-doped mesoporous TiO_2 catalyst under UV and visible light," *Journal of the Chinese Chemical Society*, vol. 59, no. 5, pp. 614–620, 2012.

[4] L. Wang and T. Egerton, "The effect of transition metal on the optical properties and photoactivity of nanoparticulate titanium dioxide," *Journal of Materials Research*, vol. 1, no. 4, pp. 19–27, 2012.

[5] D. A. Turnbull and S. G. Bishop, "Effect of transition metal co-doping on broad band luminescence excitation mechanism in rare earth-doped chalcogenide glasses," *Journal of Non-Crystalline Solids*, vol. 213, no. 214, pp. 288–294, 1997.

[6] S. Ghosh, M. Mandal, and K. Mandal, "Effects of Fe doping and FeN-codoping on magnetic properties of SnO_2 prepared by chemical co-precipitation," *Journal of Magnetism and Magnetic Materials*, vol. 323, no. 8, pp. 1083–1087, 2011.

[7] A. D. Sontakke, K. Biswas, A. K. Mandal, R. Sen, and K. Annapurna, "Iron impurity in Nd^{3+} doped phosphate laser glass-Influence on spectroscopic performance," in *Proceeding of DAE-BRNS National Laser Symposium (NLS-20)*, pp. 243–245, 2012.

[8] A. Costela, I. Garcia-Moreno, and R. Sestre:, *Handbook of Advanced Electronic and Photonic Materials and Devices*, vol. 7, Academic Press, San Diego, Calif, USA, 2001.

[9] C. F. Song, M. K. Lu, P. Yang et al., "Green emission from Cr, Dy co-doped sol–gel SiO_2 glasses," *Materials Science and Engineering B*, vol. 97, pp. 64–67, 2003.

[10] M. Genet, V. Brandel, M. P. Lahalle, and E. Simoni, "Transparent gel and xerogel of thorium phosphate. Optical spectroscopy with: Nd^{3+}, Er^{3+}, Eu^{3+}, Cr^{3+} and rhodamine 6G," in *Sol-Gel Optics*, vol. 1328 of *Proceedings of SPIE*, pp. 194–200, July 1990.

[11] M. Genet, V. Brandel, M. P. Lahalle, and E. Simoni, "Mise en evidence d'un transfert d'energie electronique entre la coumarine 460 et Eu^{3+} dans le xerogel de phosphate de thorium," *Comptes Rendus De L'Académie Des Sciences II*, vol. 311, pp. 1321–1325, 1990.

[12] K. Binnemans, "Lanthanide-based luminescent hybrid materials," *Chemical Reviews*, vol. 109, no. 9, pp. 4283–4374, 2009.

[13] W. Xu and Yi Lu, "Label-free fluorescent aptamer sensor based on regulation of malachite green fluorescence," *Analytical Chemistry*, vol. 82, no. 2, pp. 574–578, 2010.

[14] R. Reisfeld, "Theory and application of spectroscopically active glasses," in *Sol-Gel Optics*, J. D. MacKenzie and D. Ulrich, Eds., vol. 1328 of *Proceedings of SPIE*, pp. 29–39, 1990.

[15] C. J. Brinker and G. W. Scherer, Eds., *Sol-Gel Science: The Physics and Chemistry of Sol-Gel Processing*, Academic Press, New York, NY, USA, 1990.

[16] H. A. El Batal, N. A. Ghoneim, N. Abdel Shafi, and M. A. Azooz, "Infrared spectra and crystallization of some Li_2O-SiO_2 glasses and the effect of CaO, Al_2O_3 and K_2O additives," *Indian Journal of Pure and Applied Physics*, vol. 38, pp. 101–109, 2000.

[17] H. Dunken and R. H. Doremus, "Short time reactions of a na_2o-cao-sio_2 glass with water and salt solutions," *Journal of Non-Crystalline Solids*, vol. 92, no. 1, pp. 61–72, 1987.

[18] C. J. Brinker, D. R. Tallant, E. P. Roth, and C. S. Ashley, "Sol-gel transition in simple silicates. III. Structural studies during densification," *Journal of Non-Crystalline Solids*, vol. 82, no. 1-3, pp. 117–126, 1986.

[19] J. Ro Chul and J. In Chung, "Structures and properties of silica gels prepared by the sol-gel method," *Journal of Non-Crystalline Solids*, vol. 130, no. 1, pp. 8–17, 1991.

[20] D. B. Williams and C. B. Carter, *Transmission Electron Microscopy II*, Plenum Press, New York, NY, USA, 1996.

[21] I. M. Thomas, S. A. Payne, and G. D. Wilke, "Optical properties and laser demonstrations of Nd-doped sol-gel silica glasses," *Journal of Non-Crystalline Solids*, vol. 151, no. 3, pp. 183–194, 1992.

[22] M. A. Meneses-Nava, O. Barbosa-García, L. A. Díaz-Torres, S. Chávez-Cerda, M. Torres-Cisneros, and T. A. King, "Effect of PMMA impregnation on the fluorescence quantum yield of sol-gel glasses doped with quinine sulfate," *Optical Materials*, vol. 17, no. 3, pp. 415–418, 2001.

[23] T. Förster, "Experimentelle und theoretische Untersuchung des zwischenmolekularen Ubergangs von Elektronenanregungsenergie," *Zeitschrift Für Naturforschung B*, vol. 4a, article 321, 1949.

[24] D. L. Dexter, "A theory of sensitized luminescence in solids," *The Journal of Chemical Physics*, vol. 21, no. 5, pp. 836–839, 1953.

[25] C. K. Jorgensen, "Recent progress in ligand field theory," *Structure And Bonding* , vol. 1, pp. 3–121, 1966.